Chemistry and Materials Research
ISSN 2224- 3224 (Print) ISSN 2225- 0956 (Online)
Vol.12 No.4, 2020 

# The Influence of Fe , Sb doping on the Structural Properties of $SnO_2$ Powder. Comparative Study

Ahmad Khoudro[1] Samia Haj Najeeb[2]* Abeer Najjar[3]*
1.Professor, Department of Physics, Faculty of science, Tishreen University, Syria
2. MSc Student, Department of Physics, Faculty of science, Tishreen University, Syria
3. MSc Degrees, Department of Physics, Faculty of science, Tishreen University, Syria

**Abstract**
Fe , Sb doped tin oxide transparent conducting powder were prepared by solid state reaction method. Structural properties of the samples were investigated as a function of various Fe , Sb doping levels (x=0.00-0.01-0.06). The results of x-ray diffraction have shown that the samples are polycrystalline structure in tetragonal phase with preferential orientations along the (110) for all samples.The relative intensities, distance between crystalline planes (d), crystallite size (D), dislocation density (δ) and lattice parameters (a), (c).
**Keywords**: powder, Iron and Antimony doped Tin Oxide, solid state reaction, Structural properties.
**DOI:** 10.7176/CMR/12-4-01
**Publication date:** April 30th 2020

## Introduction

In recent years, there has been considerable interest in metal oxides because of their many industrial pplications, especially transparent conducting oxides (TCO). Tin oxide belongs to a transparent conductive oxide (TCO) family which are the most studied [1]. Transparent conducting oxides are semiconductors produced from a combination of metal and Oxygen. The study of SnO2 transparent conducting oxide thin films are important due to its unique attractive properties like high optical transmittance, uniformity, nontoxicity, good electrical, low resistivity, chemical inertness, stability to heat treatment, mechanical hardness, piezoelectric behavior, and its low cost. So, SnO2 is used in solar cells, sensor gas, display devices and in other important applications [2-3].

Tin Oxide is an n-type semiconductor with wide band gap energy (Eg = 3.5-4 eV) [4]. Tin Oxide has a tetragonal structure. Its unit cell contains two Tin and four Oxygen atoms as is shown in Figure 1. The Tin atom is at the center of six Oxygen atoms placed at the corners of a regular octahedron. Every Oxygen atom is surrounded by three Tin atoms at the corners of an equilateral triangle [5, 6].

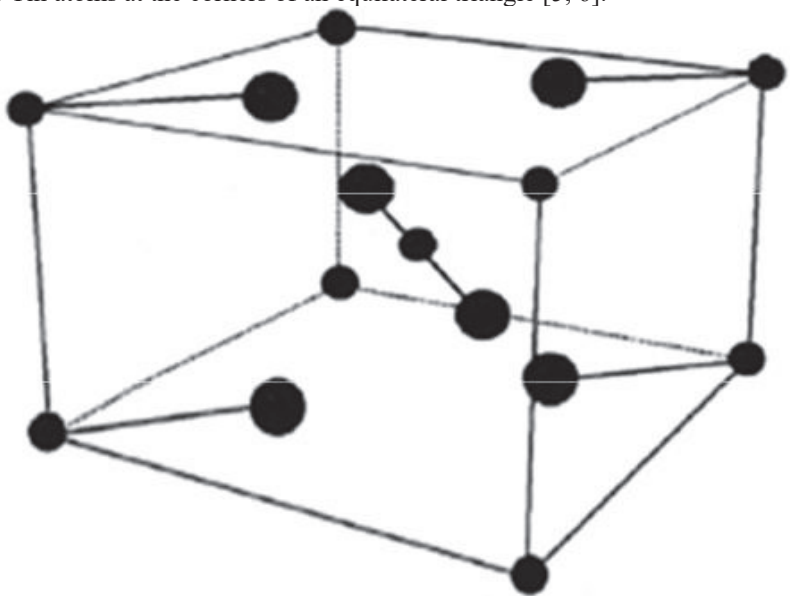

***Figure 1. Unit cell of crystalline structure of SnO2. big circles represent Oxygen atoms and small circles represent Tin atoms (from [7]).***

The structure of this material in its bulk form is tetragonal with lattice parameters of a = b = 4.737 A° and c = 3.186 °A.

## 2. Experimental Procedure

$Sn_{1-x}Fe_xO_2$ powders (x = 0.00. 0.01, 0.06) were prepared by a solid state reaction method. Were accurately weighed in required proportions and were mixed and ground thoroughly using an Agate mortar and pestle to convert to very fine powders.

 

The grinding of the mixtures was carried out for 3 hours for all the powder samples. The ground powder samples were firing at 700°C for 3 hours.

**Results and discussions**

*Structural properties*

The X-ray diffraction patterns of undoped and Fe , Sb doped $SnO_2$ powders prepared with Fe and Sb concentration 0 wt%, 1 wt% and 6 wt% are shown in Figure (1) . The XRD reveals that all samples are having polycrystalline nature with tetragonal structure which belongs to the space group P42/mnm (number136) and peaks correspond to (110) , (101) , (200) , (111) , (210) , (211) , (220) , (002) , (310) , (112) , (301) , (202) and (321) planes.

No alien phases have been observed confirming that $SnO_2$ with tetragonal cassiterite structure is the only crystalline phase appearing in both undoped and Fe , Sb doped $SnO_2$ .

The preferred orientation is (110) for all samples , but for Sb doped $SnO_2$ powders at 6 wt% doping the preferred orientation change to (101) plane .

We noticed disappearance of these orientations (111) ,(210) , (301) in Fe doped $SnO_2$ samples , and (200) , (220) , (112) in Sb doped $SnO_2$ samples .

The change in peak intensities is basically due to the replacement of $Sn^{4+}$ ions with $Fe^{3+}$ or $Sb^{5+}$ ions in the lattice of the SnO2. This process leads to the movement of $Sn^{4+}$ ions in interstitial sites , and fact that the ionic radius of tin $Sn^{4+}$ equal to ( 0.071nm) is greater than the ionic radius of $Fe^{3+}$ (0.055nm ) , and $Sb^{5+}$ ( 0.062nm) [8,9].

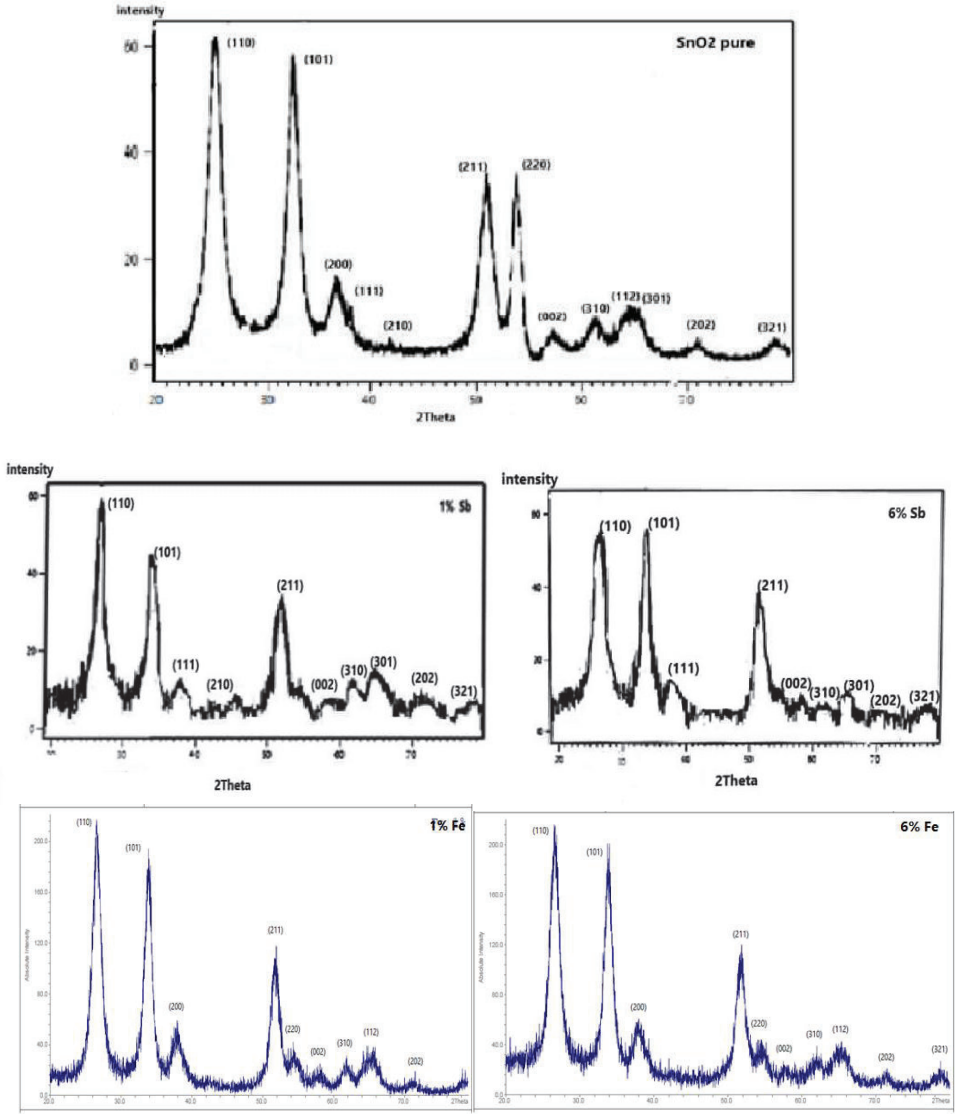


Fig (1): XRD results of pure $SnO_2$, 1 wt% Sb doped $SnO_2$, 6wt% Sb doped $SnO_2$, 1 wt% Fe doped $SnO_2$, 6 wt% Fe doped $SnO_2$.

 

Table (1) shows results of structural values of undoped $SnO_2$ sample, Fe doped $SnO_2$ samples and Sb doped $SnO_2$ samples (x=0.01-0.06) .

Table (1)

| samples | 2θ (deg) | )hkl( | d (Å) | D (nm) | Average D(nm) | δ $10^{15}$line/$m^2$ | Average δ$10^{15}$line/$m^2$ | Lattice const. a(Å) | Lattice const. c(Å) |
|---|---|---|---|---|---|---|---|---|---|
| $SnO_2$ pure | 26.62 | (110) | 3.348 | 6.128 | 11.877 | 26.628 | 14.570 | 4.733 | 3.185 |
| | 33.99 | (101) | 2.637 | 6.240 | | 25.680 | | | |
| | 37.95 | (200) | 2.370 | 9.908 | | 10.187 | | | |
| | 38.96 | (111) | 2.311 | 20.012 | | 2.497 | | | |
| | 42.62 | (210) | 2.121 | 17.471 | | 3.276 | | | |
| | 51.87 | (211) | 1.762 | 7.297 | | 18.783 | | | |
| | 54.75 | (220) | 1.676 | 18.473 | | 2.930 | | | |
| | 57.87 | (002) | 1.593 | 9.372 | | 11.385 | | | |
| | 61.99 | (310) | 1.497 | 7.221 | | 19.180 | | | |
| | 64.84 | (112) | 1.437 | 5.180 | | 37.261 | | | |
| | 65.96 | (301) | 1.416 | 15.656 | | 4.080 | | | |
| | 71.25 | (202) | 1.323 | 6.207 | | 25.955 | | | |
| | 78.30 | (321) | 1.221 | 25.240 | | 1.570 | | | |
| $SnO_2$:Fe (1wt%) | 26.50 | (110) | 3.362 | 6.202 | 7.230 | 25.994 | 21.622 | 4.755 | 3.179 |
| | 34.01 | (101) | 2.635 | 6.677 | | 22.427 | | | |
| | 37.88 | (200) | 2.375 | 5.851 | | 29.213 | | | |
| | 51.88 | (211) | 1.762 | 5.698 | | 30.803 | | | |
| | 54.38 | (220) | 1.687 | 8.332 | | 14.406 | | | |
| | 57.99 | (002) | 1.590 | 7.300 | | 18.766 | | | |
| | 61.75 | (310) | 1.502 | 9.671 | | 10.693 | | | |
| | 64.70 | (112) | 1.440 | 5.614 | | 31.726 | | | |
| | 71.25 | (202) | 1.323 | 9.724 | | 10.575 | | | |
| $SnO_2$:Fe (6wt%) | 26.54 | (110) | 3.358 | 7.615 | 8.074 | 17.244 | 18.260 | 4.748 | 3.184 |
| | 33.88 | (101) | 2.645 | 7.417 | | 18.179 | | | |
| | 37.98 | (200) | 2.368 | 7.023 | | 20.274 | | | |
| | 51.86 | (211) | 1.762 | 7.384 | | 18.341 | | | |
| | 54.56 | (220) | 1.681 | 6.226 | | 25.796 | | | |
| | 57.90 | (002) | 1.592 | 5.855 | | 29.167 | | | |
| | 62.02 | (310) | 1.496 | 7.747 | | 16.660 | | | |
| | 64.76 | (112) | 1.439 | 6.552 | | 23.293 | | | |
| | 71.34 | (202) | 1.322 | 14.189 | | 4.967 | | | |
| | 78.70 | (321) | 1.215 | 10.732 | | 8.682 | | | |
| $SnO_2$:Sb (1wt%) | 26.62 | (110) | 3.345 | 7.414 | 5.971 | 18.191 | 34.124 | 4.731 | 3.161 |
| | 33.89 | (101) | 2.642 | 5.982 | | 27.944 | | | |
| | 38.15 | (111) | 2.357 | 4.367 | | 52.415 | | | |
| | 42.51 | (210) | 2.124 | 10.857 | | 8.483 | | | |
| | 51.98 | (211) | 1.757 | 6.195 | | 26.054 | | | |
| | 58.32 | (002) | 1.580 | 5.135 | | 37.909 | | | |
| | 62.23 | (310) | 1.490 | 5.414 | | 34.111 | | | |
| | 65.36 | (301) | 1.426 | 4.073 | | 60.264 | | | |
| | 71.86 | (202) | 1.312 | 5.254 | | 36.213 | | | |
| | 78.25 | (321) | 1.220 | 5.021 | | 39.659 | | | |
| $SnO_2$:Sb (6wt%) | 26.25 | (110) | 3.392 | 5.605 | 5.186 | 31.828 | 38.356 | 4.797 | 3.150 |
| | 33.88 | (101) | 2.643 | 4.956 | | 40.706 | | | |
| | 38.02 | (111) | 2.364 | 4.718 | | 44.919 | | | |
| | 52.21 | (211) | 1.750 | 4.714 | | 44.995 | | | |
| | 58.56 | (002) | 1.575 | 5.872 | | 29.001 | | | |
| | 61.84 | (310) | 1.499 | 4.498 | | 49.414 | | | |
| | 65.15 | (301) | 1.430 | 5.967 | | 28.081 | | | |
| | 70.85 | (202) | 1.328 | 5.594 | | 31.948 | | | |
| | 78.15 | (321) | 1.222 | 4.750 | | 44.316 | | | |

 

The distance between crystalline planes values (d) are calculated by using following relation:

$$2d.\sin\theta = n\lambda \qquad (1)$$

Where d is distance between crystalline planes (A), θ is the Bragg angle, λ is the wavelength of X-rays (λ=1.54056 Å).

The crystallite size is calculated from Scherrer's equation [10]:

$$D = \frac{0.94\lambda}{\beta cos\theta} \qquad (2)$$

Where, D is the crystallite size, λ is the wavelength of X-ray, β is full width at half maximum (FWHM) intensity in radians and θ is Braggs's angle.

The dislocation density is defined as the length of dislocation lines per unit volume and calculated by following equation [11]:

$$\delta = \frac{1}{D^2} \qquad (3)$$

The lattice constants a and c for tetragonal phase structure are determined by the relation [12]:

$$\frac{1}{d^2} = \frac{h^2+k^2}{a^2} + \frac{l^2}{c^2} \qquad (4)$$

Where d and (hkl) are distance between crystalline planes and Miller indices, respectively.

The calculated lattice constants a, c values are given in table (1). It was seen that a, c and c/a match well with JCPDS card (5-467) data ( a=b= 4.737 Å and c= 3.185 Å).

Figure (2) shows the variation of the average crystallite size as a function of Sb , Fe concentration.

The average crystallite size of pure $SnO_2$ is about 11.877nm and decrease in order to 1 , 6wt% of Fe doped powders to 7.230nm , 8.074nm , respectively , while in order to 1 , 6wt% of Sb doped powders decrease to 5.971nm , 5.186nm , respectively .

We note that the greatest value of the average crystallite size is for the pure $SnO_2$ , and then decreases for the doped samples , while we notice that the lowest value is for Sb doped powders at 6wt% concentration.

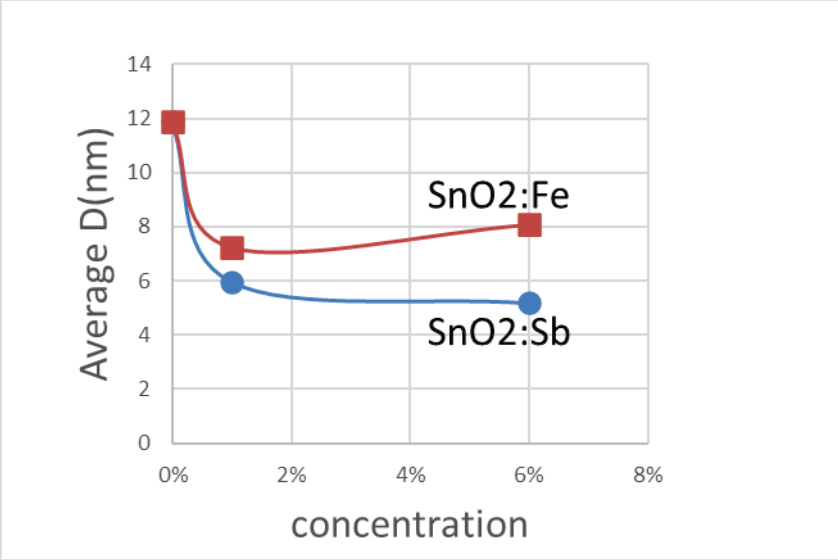


Figure (2) represents variation of the average grain size with concentrations (0wt%,1wt%,6wt% ) of Sb or Fe doped $SnO_2$ powdres.

Figure (3) shows the variation of the average dislocation density as a function of Sb , Fe concentration

The average dislocation density is about $14.570\times10^{15}$ line/$m^2$ for pure $SnO_2$ and increase in order to 1 , 6wt% of Fe doped powders to ( 21.622 , 18.260)$\times10^{15}$ line/$m^2$ , respectively , and then its value increase more in order to 1 , 6wt% of Sb doped powders to (34.124 , 38.356) $\times10^{15}$ line/$m^2$ , respectively .

Where we note that the lowest value of the average dislocation density is for pure $SnO_2$ , and then increases for doped samples and the greatest value is for Sb doped powders at 6wt% concentration .

 

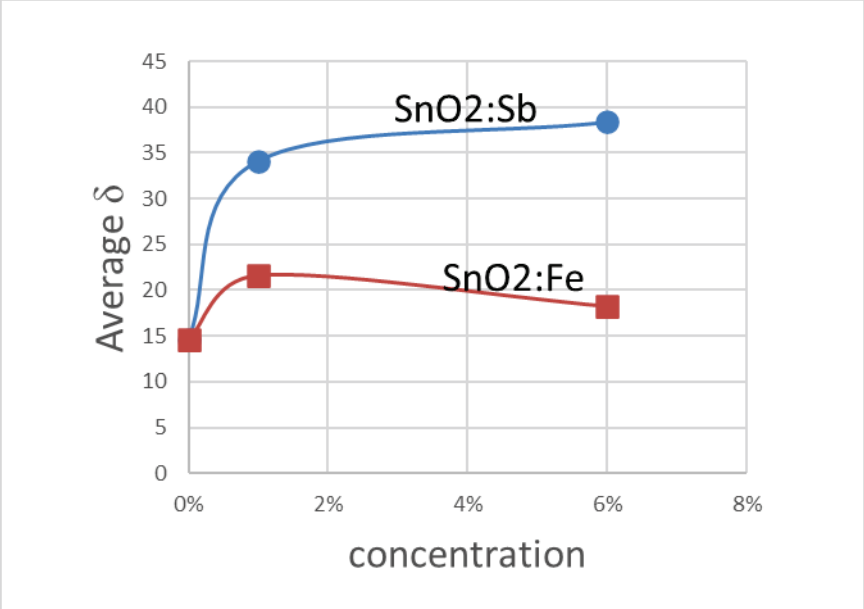


Figure (3) represents variation of the average dislocation density with concentrations (0wt%,1wt%,6wt% ) of Sb or Fe doped SnO2 powdres.

We notice from Figures 1 and 2 that the Fe doped $SnO_2$ powder with 6wt% concentration is better compared with the other doped samples because it has a greater average grain size and less dislocation density of in its crystal lattice.

## 5. Conclusion

This paper presents a study of structural properties of Sb and Fe doped $SnO_2$ powders prepared by solid state reaction method. X-ray diffraction patterns confirm that the samples have polycrystalline nature with tetragonal structure and show presence (110) ،(301) ،(202) and (321) planes in pure tin oxide sample. The preferred orientation is (110) for all samples , but for Sb doped $SnO_2$ powders at 6 wt% doping the preferred orientation change to (101) plane .We noticed disappearance of these orientations (111) ,(210) , (301) in Fe doped $SnO_2$ samples , and (200) , (220) , (112) in Sb doped $SnO_2$ samples. The average of crystallite size is within the range [11.877- 5.186 nm] for all samples. It was defined that the lattice constants a, c for all the samples, were almost identical with JCPDS values, and the ratio c/a remained constant with increasing Sb and Fe dopant concentration.

## References

[1] M. BENHALILIBA, C. E. BENOUIS, Y. S. OCAK, F. YAKUPHANOGLU (2012), "Nanostructured Al Doped SnO2 Films Grown onto ITO Substrate via Spray Pyrolysis Route",*Journal of Nano- and Electronic Physics*, Vol. 4, No. 1, pp. 1-3.

[2] S. S. ROY, J. PODDER (2010), "Synthesis and optical characterization of pure and Cu doped SnO2 thin films deposited by spray pyrolysis", *Journal of Optoelectronics and Advanced Materials*, Vol. 12, No. 7, pp. 1479-1484.

[3] TURGUT G., KESKENLER E. F., Aydin S., SONMEZ E., DOGAN S., DUZGUN B., ERTUGRUL M. (2013), "Effect of Nb Doping on Structural, Electrical and Optical Properties of Spray Deposited SnO2 Thin Films", *Super lattices and Microstructures*, 56, pp. 107-116.

[4] GANDHI T., BABU R. & RAMAMURTHI K. (2013)"Structural, Morphological, Electrical and Optical Studies of Cr Doped SnO2 Thin Films Deposited by The Spray Pyrolysis Technique", *Materials Science in Semiconductor Processing*, 16, pp. 427-479.

[5] JARZEBSKI Z. & MARTON J. (1976) "Physical Properties of SnO2 Materials", *Journal of the Electrochemical Society*, pp. 199-205.

[6] KHANAA V. & MOHANTA K. (2013) "Synthesis and Structural Characterization of SnO2 Thin Films Prepared by Spray Pyrolysis Technique", *International Journal of Advanced Research*, 1 (7), pp. 666-669.

[7] RAUL DIAZ DELGADO, "Tin Oxide Gas Sensors: An Electrochemical Approach", Ph. D Thesis, Universitat De Barcelona, 2002.

[8] M. Kuppan , S. Kaleemulla , N. Madhusudhana Rao ,N. Sai Krishna , M. Rigana Begam .D. Sreekantha Reddy . (2014) "Physical Properties of Sn1−xFexO2 Powders Using Solid State Reaction" , J Supercond Nov Magn , 27, 1315–1321.

[9] Sushant Gupta , B.C. Yadav , Praphat K.Dwivedi and B.Das . (2012) '' Structural/microstructural , optical

 

and electrical investigations of Sb-$SnO_2$ thin films deposited by spray pyrolysis'' , cond-mat.mtrl-sci .

[10] - Mariappan R., Ponnuswamy V. & Suresh P. (2012) "Effect Of Doping Concentration On The Structural And Optical Properties Of Pure And Tin Doped Zinc Oxide Thin Films By Nebulizer Spray Pyrolysis (NSP) Technique", *Superlattices and Microstructures*, 52, 500-513.

[11] - Turgut G., Keskenler E. F., Aydin S.; Sonmez E., Dogan S., Duzgun B. & Ertugrul M. (2013), "Effect Of Nb Doping On Structural, Electrical And Optical Properties Of Spray Deposited SnO2 Thin Films", *Super lattices and Microstructures*, 56, 107-116.

[12] - Gurakar S., Serin T & Serin N. (2014) "Electrical And Microstructural Properties Of (Cu, Al, In)-Doped SnO2 Films Deposited By Spray Pyrolysis", *Advanced Materials Letters*, 5(6), 309-314.